

Supplementary data:

Orienting the Heterocyclic Periphery: A Structural Basis for Chloroquine's Antimalarial Activity

Erin L. Dodd and D. Scott Bohle*

^aDepartment of Chemistry, McGill University, Montreal, H3A 0B8, Quebec, Canada

Contents:

Materials and Methods	S2
Chirality and Structure Activity Relationships in the Antimalarial Activity of Chloroquine	S4
Porphyrin numbering scheme	S5
NMR control studies -	
Job plot analysis - figure S2	S5-6
control studies - figures S3-S5	S6-9
association constants - table S1	S10
Crystallography	
details of structure	S11 - 12
crystallographic tables - table S2	S13
alterative Views of the structure - figure S6-S7	S14
Fluorescence	S15 - 16
IR	S17-18
References	S19

Materials and Methods

General Comments. Octaethylporphine and protoporphyrin IX dimethyl ester were purchased from Frontier Scientific, Inc. Gallium trichloride was purchased from STREM chemicals. Chloroquine diphosphate was purchased from Sigma-Aldrich and prepared as specified below. All other reagents were purchased from Sigma-Aldrich and used without further purification. HPLC-grade methanol, HPLC-grade dichloromethane, and double-distilled 2,6-lutidine were purchased from Sigma-Aldrich and used without further purification. NMR-grade d₄-methanol was purchased from Cambridge Isotopes and used without further purification. All single ¹H, NOESY, and ¹H titration NMR experiments were performed on a 500 MHz Varian Mercury NMR spectrometer. Infrared spectroscopy performed on an ABB Bomem MB series IR spectrometer. NMR spectra were analyzed using MestreNOVA software. Equilibrium constants determined using WinEQNMR2.¹ Gallium(III) protoporphyrin IX hydroxide synthesis and gallium(III) octaethylporphyrin chloride were prepared by literature methods.

Preparation of free base chloroquine. A quantity of the commercially available phosphate salt of the drug (500 mg to 1 g) was dissolved in water (200 mL) in a separatory funnel. Sodium hydroxide solution (1 M, 200 mL) was added until all drug precipitated. The suspension was shaken with dichloromethane (3 x 200 mL) to extract the free base drug, and organic layer separated and dried over anhydrous magnesium sulfate. The drying agent was filtered and the solvent removed in vacuo. The drug residue was dried at room temperature under high vacuum for 24-48 hours in presence of desiccant (P₂O₅).

NMR titration of gallium(III) porphyrin or acid against free-base chloroquine or structural analog of drug. All volume measurements were performed using Hamilton gastight syringes for accuracy. A solution of gallium(III) protoporphyrin IX hydroxide, gallium(III) octaethylporphyrin chloride, or propionic acid (0.020 M) is prepared in d₄-methanol (500 μL). Separately, free-base chloroquine, triethylamine, or 7-chloro-4-(1-pyrrolidinyl)quinoline (6.0 mmol) is dissolved in d₄-methanol (500 μL) in an NMR tube. Dichloromethane (2.0 μL, HPLC-grade) is added as an internal standard. Aliquots (5.0 μL or appropriate) of metalloporphyrin solution were added to the sample in the NMR tube over the course of the titration, with ¹H NMR spectra taken after 20 inversions to obtain homogeneity initially and again upon each addition. The Ga(PPIX)(OH) sample must be freshly made, kept dark, prepared immediately before use and used quickly, as some aggregation occurs over the first few hours at this concentration. NMR data were treated by non-linear fitting software WinEQNMR¹ to determine binding constants. Representative titrations are shown in Figures S3-S5 as well as in Figure 3.

Fluorescence concentration dependence of Ga(PPIX)(OH) and free-base drug. A solution (10 μM , 3.000 mL) of each compound was prepared in a 1x1x5 cm^3 Starna Q quartz fluorescence cuvette in HPLC-grade methanol, with gentle mixing to minimize oxygenation, and initial excitation and emission spectra were obtained. The excitation wavelength for each drug was chosen based upon the excitation spectrum maximum for emission at 375 nm. Serial dilution of the solution involved removal of 500 μL of cuvette solution followed by addition of 500 μL of HPLC-grade methanol, repeated 20 times. Emission spectra were obtained for each concentration. Care was taken to watch for porphyrin decomposition due to light exposure.

Fluorescence titration of Ga(PPIX)(OH) against free-base drug. All volume measurements performed using Hamilton gastight syringes for accuracy. A solution of free-base drug (0.7 μM) in HPLC-grade methanol was prepared in a fluorescence cuvette. Separately, a stock solution of Ga(PPIX)(OH) (0.5 mM) HPLC-grade methanol was prepared. An emission spectrum of the drug was taken, and subsequent emission spectra were taken upon each 5.0 μL addition of metalloporphyrin solution (to two equivalents). Mixing of solutions was gentle to minimize oxygenation and the UV spectrum was monitored to ensure no porphyrin decomposition due to singlet oxygen damage occurred.

Measurement of fluorescence lifetimes. Solutions were sparged with N_2 for 20 min. Steady-state luminescence spectra were measured using a Photon Technology International (PTI) QuantaMaster 6000 spectrofluorometer equipped with a 75 W Ushio xenon arc lamp, Czerny-Turner $f/3.4$ grating monochromators, and a Hamamatsu R-928 five-stage PMT accessory in a PTI Model 814 PMT housing with a S600 PHOTOCOOL device. UV-Vis absorbance spectra were acquired before and after to assure sample integrity.

Crystallography. Crystals of sufficient quality for diffraction were grown by adding two equivalents of racemic chloroquine free base (0.01 mmol) to a solution of gallium(III) protoporphyrin IX (0.005 mmol) in d_4 -methanol (500 μL) in an NMR tube. Ratio of reagents was verified by ^1H NMR. Sample in NMR tube was sealed with NMR tube cap and left to sit in upright in the darkest part of a cupboard (light sensitivity) undisturbed for 4 weeks in air and at room temperature. Bright pink needles were observed along the sides of the tube at that point. Crystals were sensitive to de-solvation and readily lost solvent and crystallinity, therefore they were maintained in mother liquor and harvested immediately before diffraction, placed immediately in mother liquor-infused paratone oil. Sample was held in a loop in a drop of oil frozen at 100K for diffraction. A pink needle of

GaC₅₈H₇₇ClN₇O₁₄, approximate dimensions 0.040 mm x 0.070 mm x 0.160 mm, was used for the X-ray crystallographic analysis. The X-ray intensity data were measured using a Bruker SMART APEX II Duo CCD with Cu radiation from a I μ S micro-focus source. The structure was solved and refined using the Bruker SHELXTL software package.

Concerning Chirality and Structure Activity Relationships in the Antimalarial Activity of Chloroquine

There exists considerable confusion in the literature on the chemistry and antimalarial activity of the enantiomers of chloroquine. A partial resolution, to 12% purity, was achieved in 1949² with d-bromocamphorsulfonic acid. This was found to have “no significant differences in antimalarial activity in birds and for toxicity in dogs from the racemate.” This in turn was associated with the statement in Berliner and Butler³ that the efficacies of the optical enantiomers and the racemate of chloroquine on *P. lophurae* are identical.

Subsequent workers were able to prepare the two enantiomers separately from chiral pyroglutamic acid⁴ or by separation on a chiral chromatographic phases⁵ or by resolution with 1,1'-binaphthylphosphate salts.⁶ These latter methods give specific rotations $[\alpha]_D^{22} \sim -108.5^\circ$ in ethanol for the R stereoisomer. The activity of these materials has been of some divergence as well, with Haberkorn *et al.* concluding that the d isomer was more effective in treating *P. berghei* in a mouse model at low doses, but at higher dose levels there was no significant difference between the racemate and either stereoisomer.⁷ Furthermore the authors concluded

“The results of the animal experiments thus indicate that the differences in activity between the racemate and the d-enantiomer are so small that it is not to be expected that these will be of practical importance for malarial therapy or prophylaxis in man. “

Finally, we note that more recent determinations have shown that the two stereoisomers have very similar pharmacokinetics^{8,9} and that in an in vitro model there was little difference in activity of the enantiomers and the racemate.¹⁰

Porphyrin numbering scheme

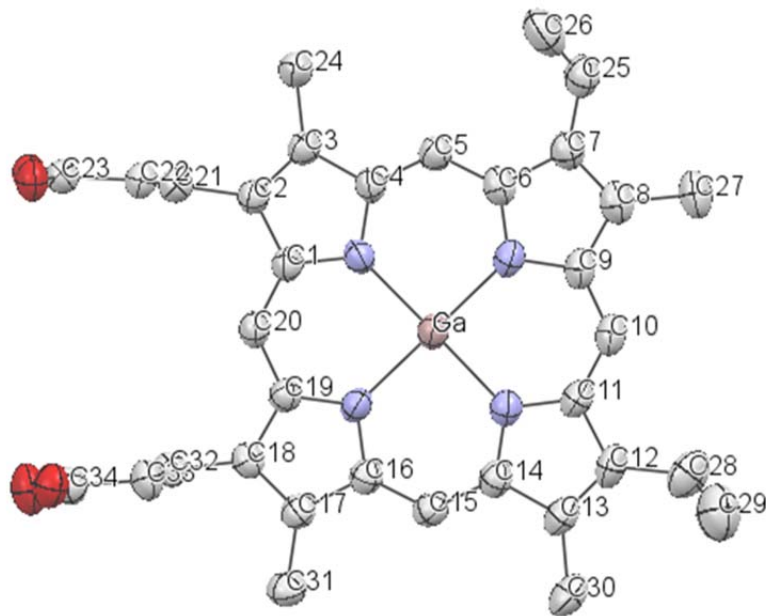


Figure S1: Porphyrin numbering scheme

NMR - further info and control studies

Equilibrium constants of simple systems under fast exchange are readily calculated from NMR titrations of simple (A + B)/AB systems with WINEQNMR, see reference 1. However there is added complexity when attempting to determine K_{eq} for multi-step pathways, especially when cooperativity is involved. Prior work has established Ga(PPIX)(X) (X = Cl⁻ or OH⁻) exists in equilibrium with its dimer in methanol solution, and that that equilibrium is itself a complicated one in which both the methoxy adduct and gallium porphyrin oligomers are formed in dynamic exchange equilibrium.^{11,12} Thus, the Job Plot analysis, Fig. S2, which fits well to a 1:1 stoichiometry, is deceiving as there are actually two binding sites per dimeric molecule, and the identification of the crystallized product as a dimer strongly suggests that the dimer structure exists in solution as well. We can determine an apparent binding constant of chloroquine to Ga(PPIX), assuming the 1:1 stoichiometry and ignoring dimerization and axial ligand exchange. However, this is at best an overestimate of what is a multi-step and possibly cooperative series of equilibria.

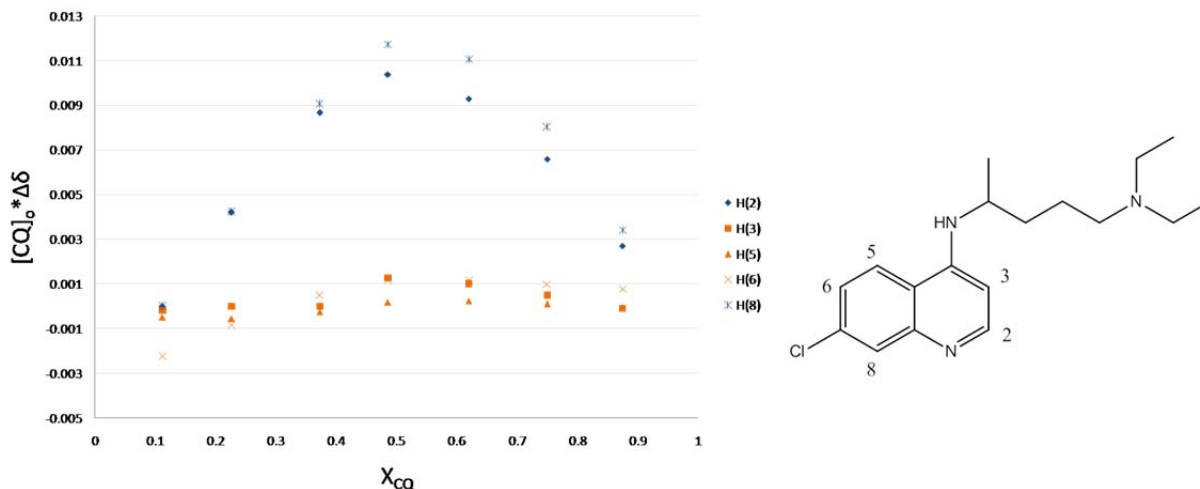


Figure S2: Job Plot based on CQ quinoline ring ^1H NMR proton shifts – analysis is consistent with a 1:1 stoichiometry. Total concentration used for acquiring Job Plot data was equal to total concentration at half point of the titration to ensure relevance and minimize aggregation effects.

The titration does not allow for differentiation to be made between monomer and dimer Ga(PPIX) species in solution, or between hydroxide vs. methoxide axial ligation, at the time of interaction with chloroquine. Cooperativity, likewise, if present, is not obvious from these plots, although the binding of the second chloroquine may well be a cooperative process which may also induce dimer formation in this soluble form. However, we can conclude that the association is medium-strong in methanol, and the structural characteristics of the binding implied by changes in ^1H NMR signal correspond very well with that seen in the solid-state crystal structure, thus we conclude that a complex of the same form exists in solution as well.

Binding of chloroquine to Ga(PPIX) involves formation of two strong hydrogen bond / proton exchange interactions: one at the quinoline N, and one at the terminal NEt_2 nitrogen. In an attempt to separate the actual binding of chloroquine into a stepwise series, we have repeated titrations against compounds that model parts of the chloroquine molecule, triethylamine (NEt_3) and 7-chloro-4-(1-pyrrolidinyl)quinoline (CPQ). A 4-aminoquinoline compound was required to mimic the basicity of the chloroquine ring nitrogen.¹³ Proton exchange was observed, as well as large upfield shifts in the protons nearest the N-face of the quinoline as seen in chloroquine. The comparison allows us to see that the interaction of gallium protoporphyrin IX with chloroquine leads to larger peak displacement in the NMR signal at similar concentrations than that induced in either free base or side chain-free 4-aminoquinoline. More importantly, the similarity in ^1H NMR shift patterns suggests structural re-arrangements that are induced by each of the two parts of the chloroquine molecule are consistent with what is observed with each ‘part’ on its own.

The dependence of the binding strength on the structure of the porphyrin as a single unit, as compared to either of its ‘parts’ in isolated systems, was also explored. Propionic acid induces a large displacement of the chloroquine terminal amino ethyl proton shifts without upfield shift of the quinoline ring protons, even at large excess of propionic acid. The synthetic porphyrin compound gallium(III) octaethylporphyrin (OEP), which differs from protoporphyrin IX in functionality, lacking any carboxylic acid-containing side chains, induces the same pattern of upfield shift in the ^1H NMR signals of the protons on the N-face of the quinoline ring of chloroquine, but with smaller peak displacement and without noticeable broadening. Shifts in the proton signals of the chloroquine end chains also follow the same pattern of directional movement, but the displacements are much smaller and no broadening is seen.

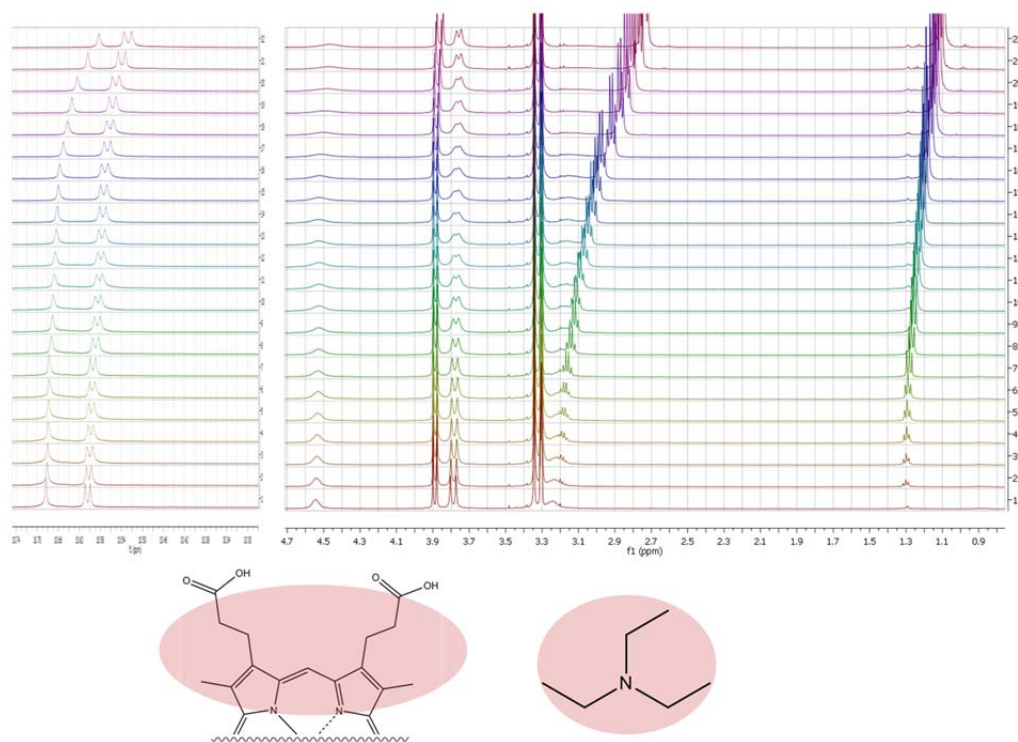


Figure S3. Stacked ^1H NMR spectra - Affected regions of spectra when NEt_3 is titrated into Ga(PPIX)(OH) (titration beginning – bottom of stack; end – top). Note broadening in porphyrin peaks, downfield shifts of NEt_3 peaks at high gallium porphyrin : NEt_3 ratio. Affected portions of molecules circled in red.

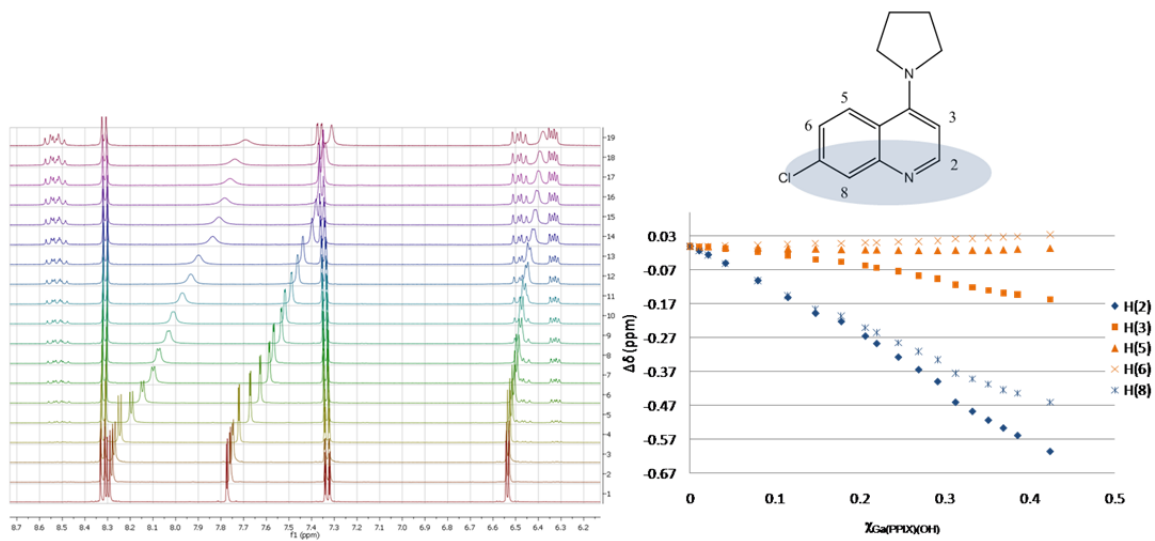


Figure S4 plot of $\Delta\delta$ of CPQ quinoline ring peaks with increasing Ga(PPIX) concentration alongside stacked spectra (increasing [Ga(PPIX)(OH)] towards the top), demonstrating change in local chemical environment for quinoline ring protons H(2) and H(8), shown in blue points.

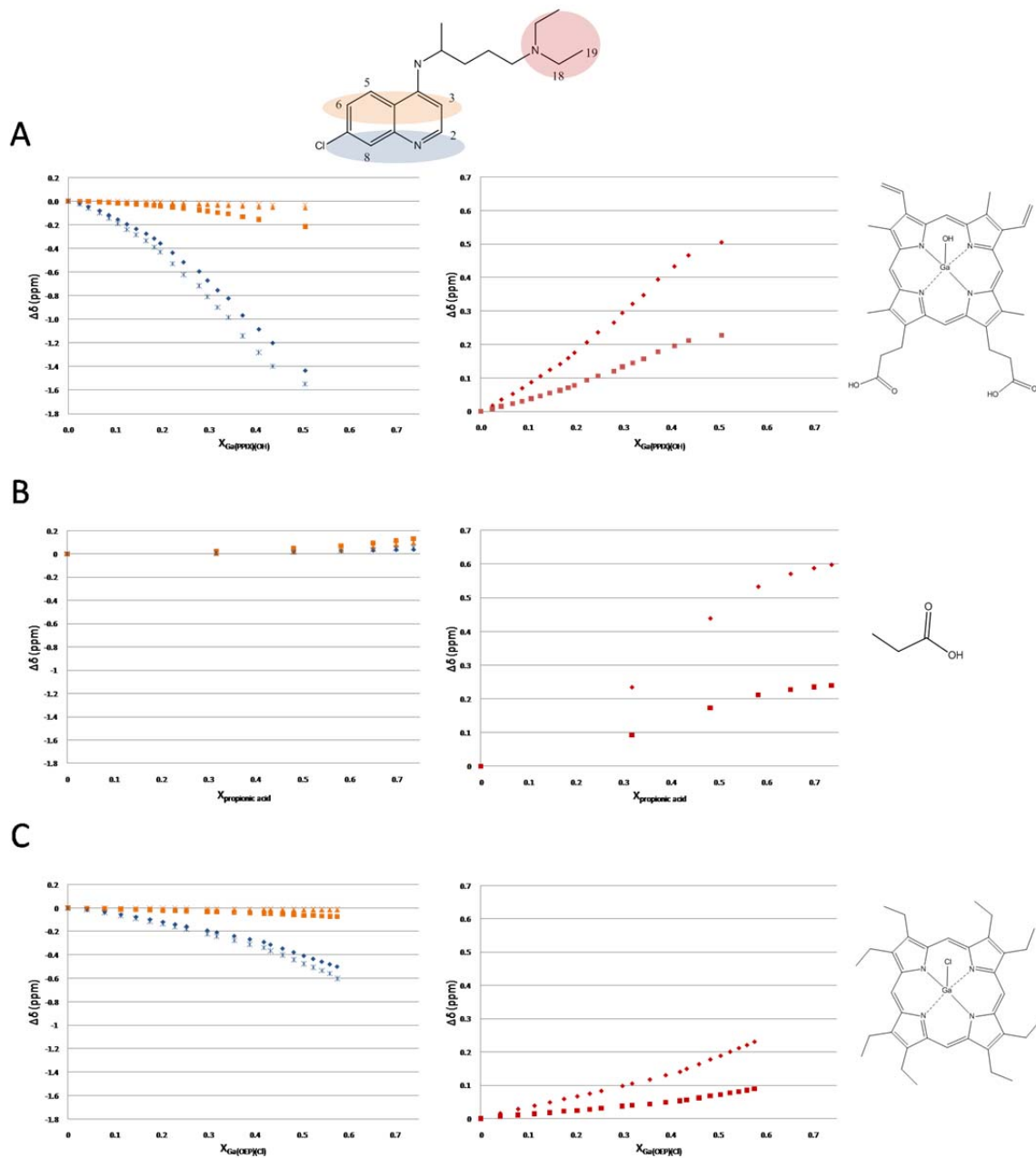


Figure S5 peak shift for quinoline ring region (left) and terminal amine region (right) of the chloroquine spectrum (for near-equal starting concentrations of chloroquine) upon adding **A.** Ga(PPIX)(OH) - shows maximal displacement in both regions; **B.** propionic acid (PA) – displacement only in the terminal amine region; **C.** Ga(OEP)(Cl) – slight displacement in both regions. Data for each chloroquine regions is color-coded (red - terminal amine ethyl groups; blue - quinoline H(2), H(8) region of quinoline-porphyrin ring current interaction in A and C; orange – quinoline protons H(3), H(5), H(6)).

Table S1: Association constants

base	pK _a of conjugate acid	porphyrin	K _{association} by NMR (M ⁻¹)
Et ₃ N	11	Ga(PPIX)(OH)	2.80 +/- 0.13 x 10 ^{+3a} ; 2.40 +/- 0.16 x 10 ^{+3b}
CPQ	8.5 ^c	Ga(PPIX)(OH)	3.4 +/- 0.5 x 10 ⁺³
chloroquine free base ¹⁴	9.94 ^d ; 8.10 ^e	Ga(PPIX)(OH)	1.48 +/- 0.05 x 10 ⁺⁴
chloroquine free base		Ga(OEP)OH	3.79 +/- 0.17 x 10 ⁺²
chloroquine free base		propionic acid	9.2 +/- 0.2 x 10 ⁺²

* a – first deprotonation; b – second deprotonation; c – predicted based on pK_a of the ring N of 4-aminoquinoine¹³; d - terminal diethylamino N; e - quinoline ring N. Binding constants determined using the program WINEQNMR¹ All calculations involving protoporphyrin IX species are based on an assumption of each porphyrin unit acting as monomer, and are thus estimates which disregard the complexities of dimerization and/or cooperativity.

Crystallography

The reciprocal dimer of gallium(III) protoporphyrin IX spontaneously forms in methanol solution containing monomeric gallium(III) protoporphyrin IX hydroxide and two equivalents of chloroquine free base, and crystallizes as a 6-coordinate gallium porphyrin-drug complex in space group C2/c with one drug molecule for each metalloporphyrin unit. Both enantiomers of the drug are present in the structure, and are related by inversion symmetry. The structure confirms that chloroquine binds to the dimer via non-covalent interactions which are dominated by hydrogen bonding and weaker Van der Waals forces, and that it stabilizes the dimer in a 6-coordinate structure.

Needle-shaped crystals of the drug-dimer complex suitable for x-ray diffraction grow well in methanol solutions containing ratios of two or more molecules of racemic free base chloroquine per molecule of Ga(PPIX)(OH). The structure of the drug-metalloporphyrin complex, Figure 2A, has an extensive hydrogen bonding and solvation network, Figure S2, and the complex exists as a zwitterion as predicted by the pKa's of the combined acidic and basic functional groups. In Figure 2B N(7) is protonated and engaged in a hydrogen bond (2.685 Å) with the 'free' oxygen of the monohapto-bound carboxylate. Both C-O bonds of the metal-bound carboxylate group are of nearly equal length. On the far side of each 6-coordinate gallium atom, at a marginally longer bond length, the oxygen atom of a methanol molecule is bound which shares a proton with the quinoline ring nitrogen N(5) at an O-N distance of 2.669 Å. The Ga-O bond lengths are in contrast to the pyridine dimer reported previously, in which the Ga-N axial bond length is significantly longer.¹¹ In that structure there is a similar hydrogen bonding network, however in the drug-dimer complex structure the hydrogen bonding is largely inter- rather than intra- molecular, with the chloroquine diethylamino N replacing the free propionic acid group in binding the far oxygen of the bound propionate and thus stabilizing the 6-coordinate structure.

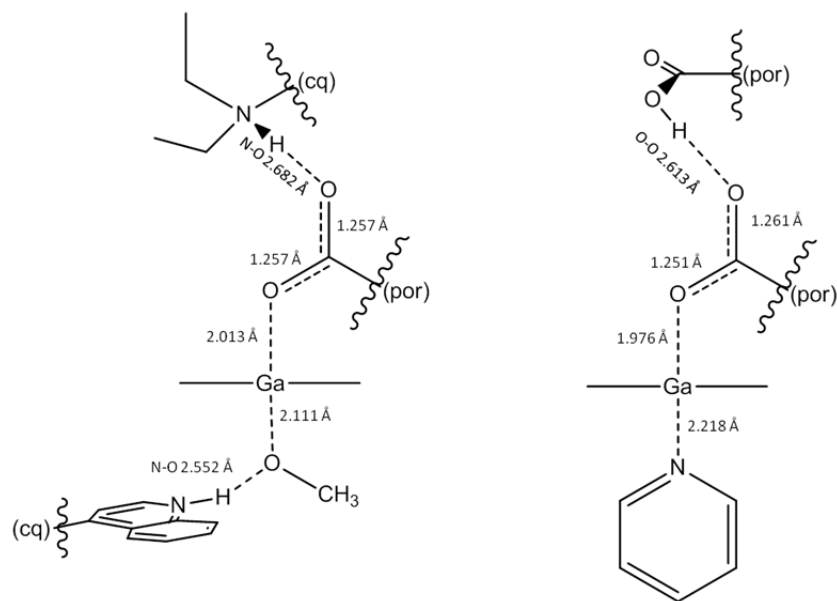


Figure S 6: Hydrogen bonding of the chloroquine extended chain with the bound carboxylate of the dimer (left); intra-dimer hydrogen bond between carboxylates of the same porphyrin in $[\text{Ga}(\text{PPIX})(\text{py})]_2 \cdot \text{py}^{11}$ (right)

The 6-coordinate solvent coordinated structures are possibly important for their solubility since hemozoin and its gallium analog¹⁵ are insoluble and inert, and both this complex and related 6-coordinate dimers of this compound¹¹ are readily soluble in methanol. The differing interactions of the free propionate groups also contribute to the differing solubility. Hemozoin itself is linked across porphyrin dimer units by hydrogen bonding between the free propionates extended to either side of each dimer unit; in the 6-coordinate cases, other hydrogen bonding pairing prevail as the sixth ligand makes staggered packing in the unit cell more favorable and thus puts the free propionic acid groups too far apart to interact.

Table S2: Sample and Crystal Data for 1

Chemical formula	C ₅₈ H ₇₇ ClGa ₇ N ₇ O ₁₄	
Formula weight	1201.44	
Temperature	112(2) K	
Wavelength	1.54178 Å	
Crystal size	0.040 x 0.070 x 0.160 mm	
Crystal habit	pink needle	
Crystal system	monoclinic	
Space group	C2/c	
Unit cell dimensions	a = 29.9311(9) Å	α = 90°
	b = 14.6378(3) Å	β = 98.328(2)°
	c = 28.7485(6) Å	γ = 90°
Volume	12462.6(5) Å ³	
Z	8	
Density (calculated)	1.281 Mg/cm ³	
Absorption coefficient	1.551 mm ⁻¹	
F(000)	5072	
Theta range for data collection	2.98 to 44.52°	
Index ranges	-27<=h<=27, -13<=k<=13, -26<=l<=26	
Reflections collected	29279	
Independent reflections	4909 [R(int) = 0.0804]	
Coverage of independent reflections	100.00%	
Absorption correction	multi-scan	
Max. and min. transmission	0.9349 and 0.7917	
Structure solution technique	direct methods	
Structure solution program	SHELXS-97 (Sheldrick, 2008)	
Refinement method	Full-matrix least-squares on F ²	
Refinement program	SHELXL-97 (Sheldrick, 2008)	
Function minimized	Σ w(F _o ² - F _c ²) ²	
Data / restraints / parameters	4909 / 52 / 725	
Goodness-of-fit on F²	1.021	
Δ/σ_{max}	2.393	
Final R indices	3553 data; I>2σ(I)	R1 = 0.0682, wR2 = 0.1778
	all data	R1 = 0.0967, wR2 = 0.1974
Weighting scheme	w=1/[σ ² (F _o ²)+(0.1106P) ² +0.7426P] where P=(F _o ² +2F _c ²)/3	
Largest diff. peak and hole	0.107 and -0.044 eÅ ⁻³	
R.M.S. deviation from mean	0.007 eÅ ⁻³	

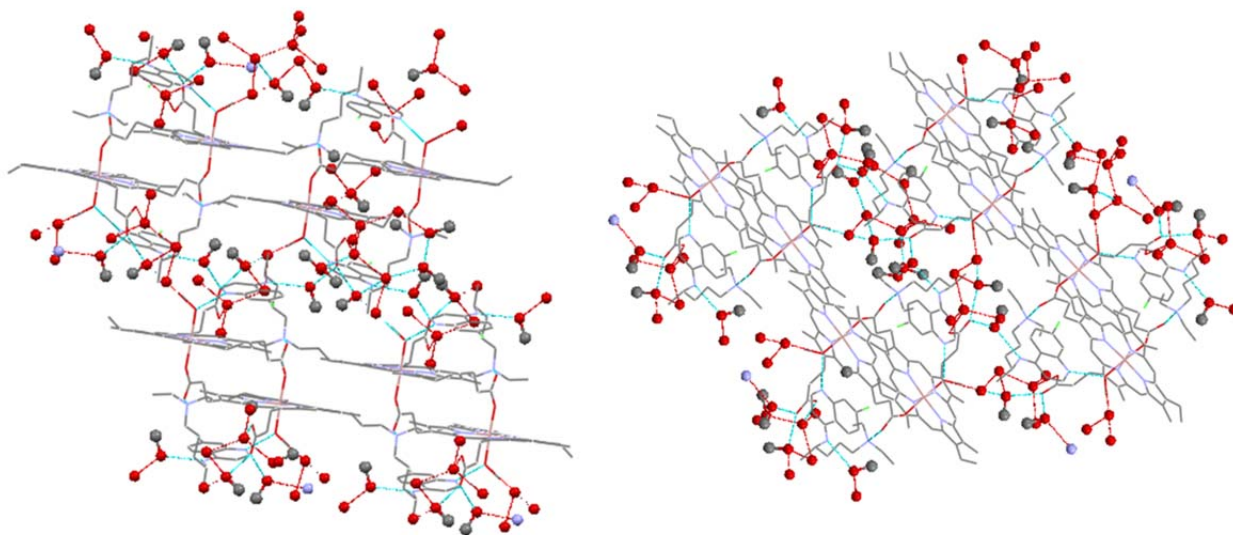


Figure S7: a network of solvated water and methanol molecules connected by hydrogen bonds and the free propionates of the porphyrin dimers. Hydrogen bonds depicted as dashed cyan lines.

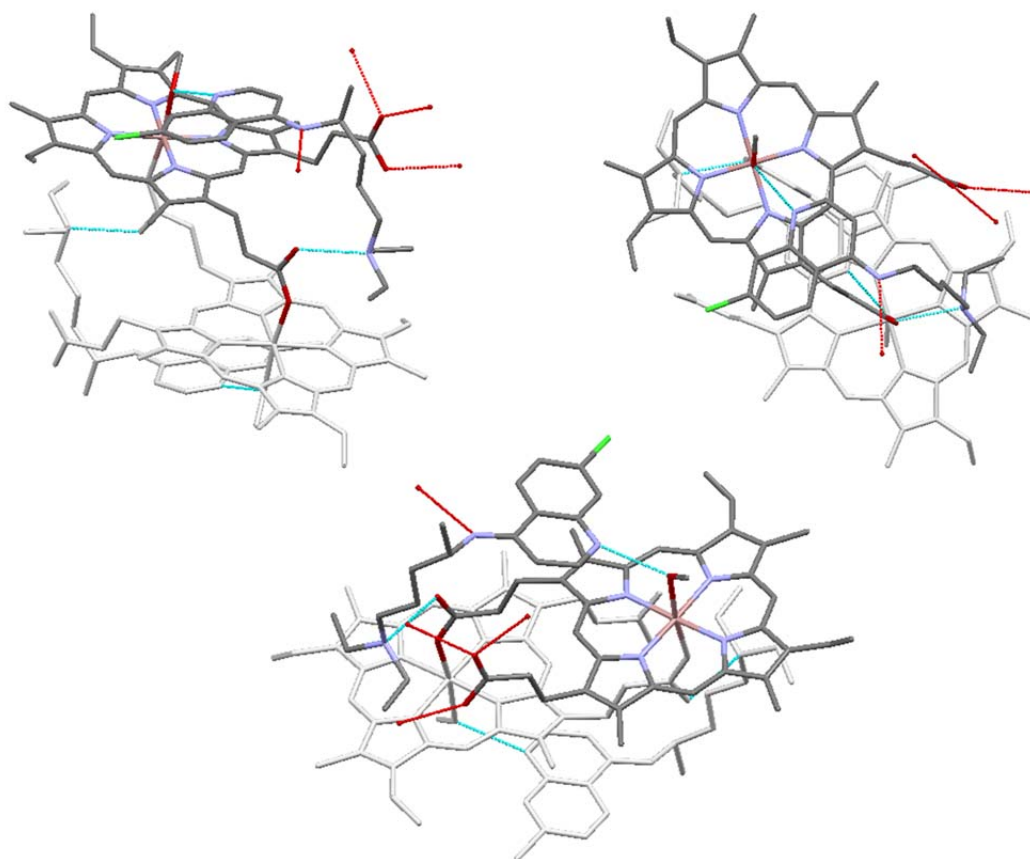


Figure S8: Hydrogen bonding connectivity of the core dimer complex to solvent molecules

Fluorescence

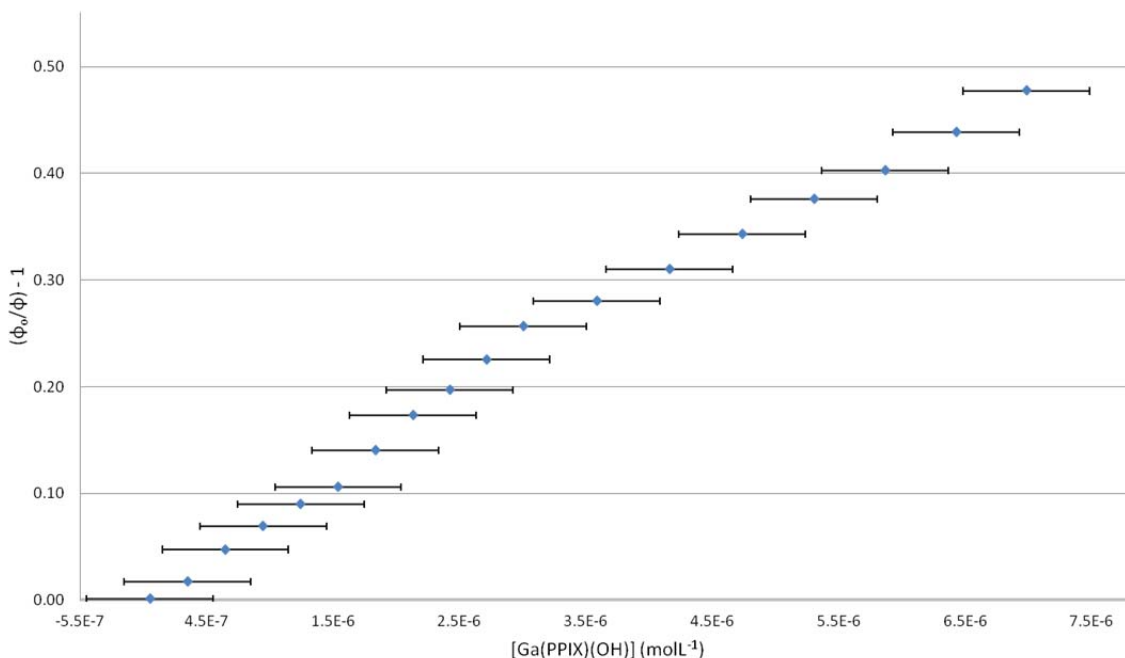


Figure S9: Stern-Volmer treatment for reaction equilibrium constant determination at 373nm, $\frac{\phi_0}{\phi} = 1 + K_{eq}[Ga(PPIX)(OH)]$

A variety of studies determining the binding/ π -stacking of small aromatic molecules to synthetic porphyrins have been done in the past using fluorescence emission techniques¹⁶ and an early study quantified the quenching of chloroquine fluorescence by hemin.¹⁷ The fluorescence emission spectrum of quinoline molecules is complex, with excitation at 330 nm yielding several overlapped peaks that appear as one with an apparent maximum of 365 nm.¹⁸ Presence of an alcohol, especially as solvent, will generate an increase in chloroquine emission intensity through a hydrogen bonding interaction through the quinoline nitrogen.¹⁸⁻²¹

There is not sufficient evidence to verify the extent of contribution of Förster Resonance Energy Transfer (FRET) in this system, which would have been expected for a π -stacked complex. However the intensity decrease is quite telling, and matches our predictions based on the solid state structure whose N-

bound alcohol is also bound to the gallium. Porphyrin Q-band emissions would be seen in the presence or absence of FRET effects because porphyrin excitation is possible over a long range of wavelengths, with the photoexcitation event leading to a sequence of non-emissive excitation energy decreases, culminating in emission in the low-energy region of the spectrum. The increase in intensity of the Q-band emissions may be due to charge transfer,^{22,23} FRET, or to a magnification of the alcohol-mediated stabilization of the chloroquine emissive state. Work is ongoing to verify the source of the fluorescence behavior. Our lab is currently engaged in ongoing work towards the determination of exact stoichiometry and the degree of cooperativity in the system.

IR

We were curious as to whether the crystalline material would maintain its structure in the absence of the solvate molecules. A sample of crystalline materials from the same batch that provided the crystal for diffraction was towel-dried, ground and pressed into a potassium bromide pellet for IR. The same KBr pellet was dried *in vacuo* for five days and its IR spectra measured every twenty-four hours. A significant decrease in solvent peak at 3440 cm^{-1} was observed (Figure 4 - 6), but the remainder of the spectrum did not show shifts of more than 1 cm^{-1} , save for one band. The initial spectrum contained a $\nu_{\text{asym}}(\text{CO}_2)$ peak at 1614 cm^{-1} with a shoulder at 1631 cm^{-1} , as well as a more intense $\nu_{\text{asym}}(\text{CO}_2)$ peak at 1577 cm^{-1} which did not shift significantly, but within the first 24 hrs that had decreased to a sharper, much less intense signal at 1609 cm^{-1} . This shift is small but suggests that one carboxylate does experience a slight change of chemical environment within the solid, though the remainder of the molecule experiences little to no change. The crystallographic data obtained confirmed that in the crystalline state the free carboxylate was hydrogen-bonded to the solvent network, while the gallium-bound carboxylate was engaged in hydrogen bonding with only the drug. Therefore the 1614 cm^{-1} $\nu_{\text{asym}}(\text{CO}_2)$ band is assigned as that of the free carboxylate, and the intense 1577 cm^{-1} $\nu_{\text{asym}}(\text{CO}_2)$ band as that of the gallium-bound carboxylate. The respective $\nu_{\text{sym}}(\text{CO}_2)$ bands are found at 1451 cm^{-1} and 1384 cm^{-1} .

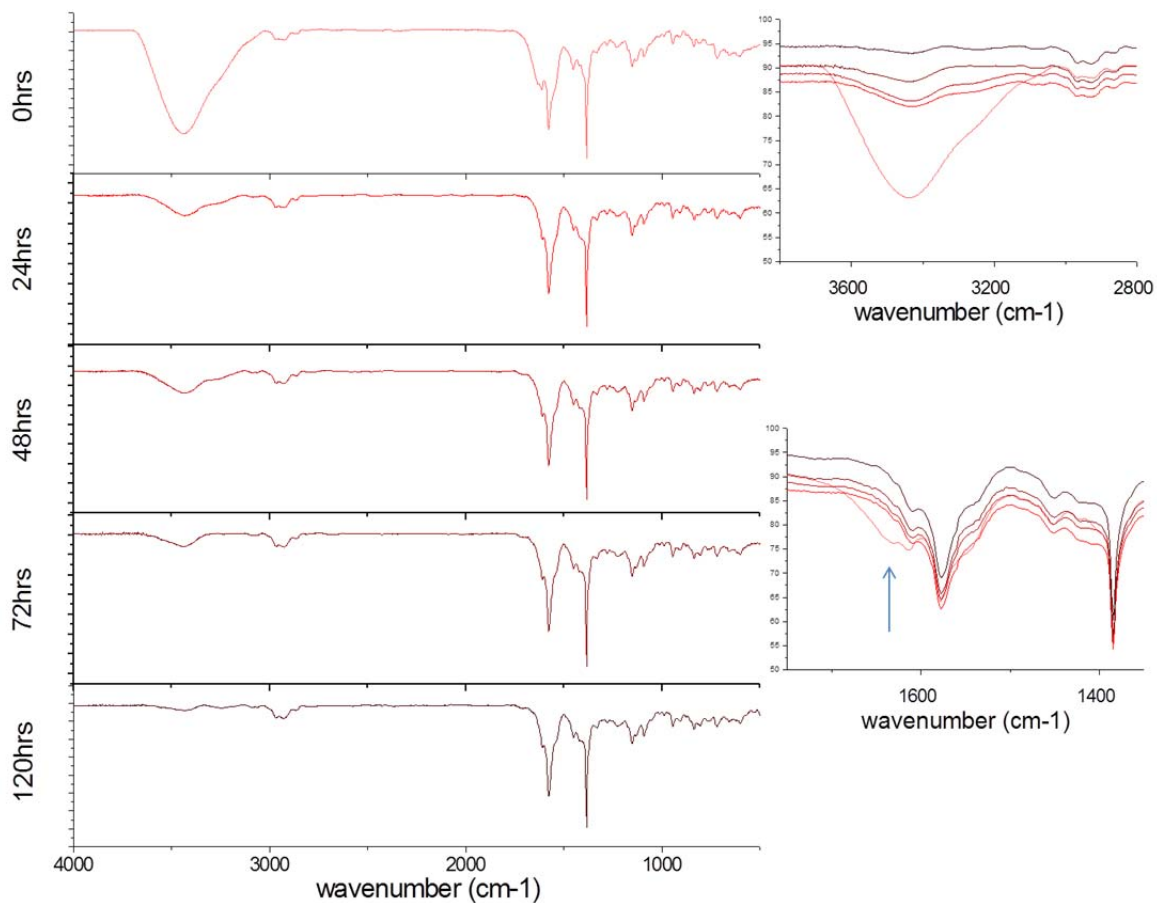


Figure S10 Stacked IR spectra for crystalline 1 showing spectral changes on solvate removal. Sample was isolated from the same batch which produced the crystal for diffraction. a. fresh from mother liquor; b. dried *in vacuo* 24hrs; c. dried *in vacuo* 48hrs; d. dried *in vacuo* 72hrs; e. dried *in vacuo* 5 days. Note the shrinking and shifting of the band at 1631 cm^{-1} (see arrow).

References

- (1) Hynes, M. J. *Journal of the Chemical Society, Dalton Transactions* **1993**, 311.
- (2) Riegel, B.; Sherwood, L. T. J. *Journal of the American Chemical Society* **1949**, *71*, 1129.
- (3) Berliner, R. T.; Butler, T. In *Survey of Antimalarial drugs, 1941-1945*; Wiselogle, F. Y., Edwards, J. V., Eds.; U. Michigan: Ann Arbor, 1946, p 221.
- (4) Blauer, G.; Akkawi, M.; Fleischhacker, W.; Hiessboeck, R. *Chirality* **1998**, *10*, 556.
- (5) Blaschke, G.; Kraft, H. P.; Schwanghart, A. D. *Chem. Ber.* **1978**, *111*, 2732.
- (6) Craig, J. C.; Ansari, A. M. *Chirality* **1993**, *5*, 188.
- (7) Haberkorn, A.; Kraft, H. P.; Blaschke, G. *Tropenmed. Parast.* **1979**, *30*, 308.
- (8) Brocks, D. R.; Mehvar, R. *Clinical Pharmacokinetics* **2003**, *42*, 1359.
- (9) Brocks, D. R.; Vakily, M.; Mehvar, R. *Chirality in Drug Design and Development* **2004**, 191.
- (10) Fu, S.; Bjorkman, A.; Wahlin, B.; Ofori-Adjei, D.; Ericsson O; Sjoqvist, F. *Br. J. Clin. Pharmacol.* **1986**, *22*, 93.
- (11) Bohle, D. S.; Dodd, E. L. *Inorg. Chem.* **2012**, *51*, 4411.
- (12) Bohle, D. S.; Dodd Erin, L.; Pinter, T. B. J.; Stillman, M. J. *Inorg. Chem.* **2012**, *51*.
- (13) Albert, A.; Goldacre, R. *Nature (London, U. K.)* **1944**, *153*, 467.
- (14) Hong, D. D. In *Analytical Profiles of Drug Substances*; Klaus, F., Ed.; Academic Press: 1976; Vol. Volume 5, p 61.
- (15) Bohle, D. S.; Dodd, E. L.; Pinter, T. B. J.; Stillman, M. J. *Inorganic Chemistry* **2012**.
- (16) Schneider, H.-J.; Wang, M. J. *Org. Chem.* **1994**, *59*, 7464.
- (17) Panijpan, B.; Mohan Rao, C.; Balasubramanian, D. *Biosci. Rep.* **1983**, *3*, 1113.
- (18) Anton, M. F.; Nicol, M. J. *Lumin.* **1979**, *18-19*, 131.
- (19) Safarzadeh-Amiri, A. *J. Phys. Chem.* **1989**, *93*, 4999.
- (20) Aaron, J.-J.; Fidanza, J. *Talanta* **1982**, *29*, 383.
- (21) Moomaw, W. R.; Anton, M. F. *J. Phys. Chem* **1976**, *80*.
- (22) Barbara, P. F.; Meyer, T. J.; Ratner, M. A. *J. Phys. Chem* **1996**, *100*, 13148.
- (23) Eng, M. P.; Albinsson, B. *Angew. Chem. Int. Ed. Engl.* **2006**, *45*.